Sprays Formed by Flashing Liquid Jets

RALPH BROWN and J. LOUIS YORK

University of Michigan, Ann Arbor, Michigan

Liquids forced from a high-pressure zone into a low-pressure zone often cross the equilibrium pressure for the liquid temperature and disintegrate into a spray by partial evolution of vapor. The ordinary aerosol dispenser is a common example of this operation, and flash boiling is another.

This paper reports on a study of the sprays formed by such a process and of the mechanism of spray formation. Sprays from water and Freon-11 jets were analyzed for drop sizes, drop velocities, and spray patterns. The breakup mechanism was analyzed and data presented to show some of the controlling factors.

A critical superheat was found, above which the jet of liquid is shattered by rapid bubble growth within it. The bubble-growth rate was correlated with the Weber number, and a critical value of the Weber number was found to be 12.5 for low-viscosity liquids. The mean drop size was also correlated with Weber number and degree of superheat.

The spray from rough orifices and sharp-edged orifices was compared with sprays produced from cold liquids by other techniques and was found to be comparable in all respects except temperature.

Liquids moving isothermally from a high-pressure zone to a low-pressure zone may cross the bubble-point curve, attaining final equilibrium wholly or in part as a vapor. This action has long been the basis for flash evaporation and for pressure dispensing of aerosols, such as insecticides, hair sprays, and many other household materials. Thermodynamic studies of the process have been made, but practically nothing appears in the literature regarding the physical process of disintegration of the liquid mass into drops and vapor.

This paper reports on a study of the mechanism of spray formation by flashing of a cylindrical jet and on the spray formed by this process (*1*). Experimental techniques include high-speed photography of the breakup zone and of the spray, with drop sizes and velocities computed from a photographic analytical procedure. Most of the data are for superheated water injected into the room atmosphere, but some data on Freon-11 (trichloromonofluoromethane) are considered.

The voluminous literature on sprays includes a reasonable number of articles on mechanism of spray formation, but all of these describe systems for which aerodynamic forces and surface tension are the key forces in disintegration. The range of flow rates, velocities, and stream sizes employed in this study provides poor spray formation with cold water as the liquid medium, but a satisfactory spray with superheated water. This indicates that the normal relationships of dimensionless groups and variables is not effective when bulk vaporization is a factor in the spray formation. Many of these relationships were examined with the data from flashing jets in an attempt to organize and to explain the data, and some were helpful.

Rayleigh (*2*) analyzed the instability of liquid jets which disintegrated by surface tension forces, and Weber (*3*) extended the analysis to include aerodynamic forces. Weber found that the magnitude of the disruption increases with a dimensionless number, now called the *Weber number*, one form of which is

$$N_{We} = \frac{\rho_g V^2 d}{2g_c \sigma}$$

The Weber number may be considered as the ratio of the impact stress of the gas phase on the interface to the normal stress caused by the interfacial tension acting on any cross section. For low-viscosity fluids the type of disintegration depends upon the Weber number (*4*). When $N_{We} < 0.2$, only the pinching-off action of interfacial tension applies; from $0.2 < N_{We} < 8$, the action is a sinuous distortion which whips the jet into segments; and for $N_{We} > 8$, the action is more violent with ligaments of fluid separating from the jet and atomization occurring. At even higher Weber numbers the masses and drops of liquid formed originally from the main jet will themselves be broken up still further; that is secondary atomization will occur.

Thermodynamically, flashing results from suddenly lowering the pressure on a liquid until the bubble point is reached. Further lowering of the pressure will leave the liquid superheated or at a temperature higher than the saturation temperature corresponding to the pressure, and the liquid tends to convert to a vapor to regain equilibrium. Under adiabatic conditions the vapor formed can obtain its latent heat of vaporization only at the expense of the sensible heat of the remaining liquid. Equilibrium will be reached when the fraction of liquid converted to vapor has extracted enough energy from the residual liquid to cool the two phases to the saturation or equilibrium temperature.

Flashing can also occur when a solution of gas in liquid is suddenly reduced in pressure below the bubble point. As the gas comes out of solution, it will require heat which can come only from cooling of the residual liquid. When the phase change has restored equilibrium, the process ceases.

The generation of vapor in either case is not restricted to the surface of

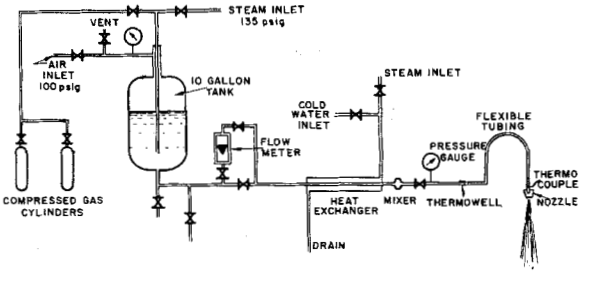

Fig. 1. Liquid injection system.

Ralph Brown is with Scott Paper Company, Philadelphia, Pennsylvania.

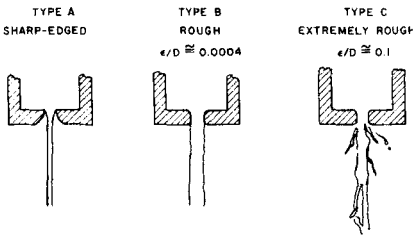

Fig. 2. Experimental nozzle types.

the liquid phase but can originate at any suitable nucleus in the liquid phase. After initial nucleation of the bubbles the gas will be more likely to form at the bubble surfaces, causing rapid growth of the bubble and a corresponding physical displacement of the adjacent liquid. The displacement can cause disintegration of unconfined liquid, analogous to that resulting from bumping of superheated liquid in boiling flasks.

EXPERIMENTAL EQUIPMENT

Flashing can occur in any configuration of liquid, either lying quiescent in a pressure tank or being ejected through some nozzle configuration into a low-pressure region. In an attempt to simplify the geometrical system this study was conducted on cylindrical jets issuing from simple circular openings, with no effort to induce swirl, twist, or internal turbulence in addition to that which is acquired by flow through ordinary tubing.

Figure 1 shows the general piping diagram. The pressure tank could be operated with steam pressurization on hot water or air or gas pressurization on other fluids. The heat exchanger could be operated as a heater or cooler to control the liquid temperature fed to the nozzle. Maximum pressure on the system was about 300 lb./sq. in., but this was rarely employed, as the purpose of flash spraying is to reduce the pressures needed to produce a good spray.

The three types of nozzles employed are shown in Figure 2 and described in Table 1. Type A was a sharp-edged orifice and gave a smooth-surface jet with cold water, which was stable for more than 100 jet diameters and then disintegrated by surface-tension action as discussed by Rayleigh (2). Type B was a drilled hole with a length-to-diameter ratio of about 1.0 and a roughness of about 20 μ in. It delivered a rough-surfaced jet with cold water, appearing turbulent but being quite stable for several hundred diameters before eventually disintegrating by surface-tension action. Type C was a nozzle of Type B with glass beads (170 to 200 mesh) cemented in the nozzle orifice to provide an extremely rough surface. With cold water Type C gave a ragged stream with ligaments torn from the main jet as it emerged from the orifice.

Table 1. Description of Nozzles

Type	Diameter, in.	Length, in.	L/D	Roughness (μin. RMS)	ϵ/D
A	0.030	0.030	1	—	—
A	0.040	0.040	1	—	—
A	0.080	0.080	1	—	—
B	0.020	0.020	1	—	0.0004 (est.)
B	0.031	0.025	0.8	—	0.0004 (est.)
B	0.040	0.035	0.9	14 ± 1	0.00035
B	0.060	0.054	0.9	25 ± 1	0.00042
C	0.020	0.057	3	3000	0.12

Table 2. Minimum Initial Radius for Bubble Growth in Water Under 1 Atm.

r_o (μ)	2.90	0.605	0.470	0.378	0.300	0.245	0.201
T_o (°F.)	220	266	275	284	293	302	311

Three liquids were sprayed: water, Freon-11, and water through which carbon dioxide gas had been bubbled for 20 min. at 90 lb./sq. in. Practically all runs discussed here were with water.

The breakup zone and the spray were studied by high-speed silhouette photography (5). Light flashes of about 1 μ sec. duration were delivered. Photographs were taken with a magnification of 10 X. Velocity measurements were made by double exposures with a time interval of 22.4 μ sec. between the two exposures. The distance between two images of a drop gave one component of its velocity.

Spray analyses were made on images of the negatives projected onto a ground-glass screen at 10 X, a total magnification of 100 X. Then the drop images were counted into size classes from which the distribution could be shown and the average sizes calculated. The depth of field and the associated degree of blur of the images in each size class was known; therefore the count was for the drops in a known volume of spray. By multiplying the number of each size by the average velocity of that size a weighted average resulted which corresponded to the distribution of drops moving through the sample volume in a unit time.

JET BREAKUP

Operation of the equipment at a constant flow rate and increasingly higher liquid temperatures shows that significant flashing does not occur at temperatures just above the saturation temperature, but that a substantial increase above saturation must be provided. The temperatures below which no effect is shown on the jet and above which the jet is shattered by flashing are in a narrow range of about 5°F. for each flow rate in each nozzle, although the limiting temperatures shift in absolute value for each change in variable. The *shattering temperature* is the name given to the mean value of the limits between no significant effect on the jet and rather complete disintegration of the jet. Data on the sprays produced showed little gain in breakup of the jet by further increases in the temperature; thus the shattering temperature indicates a unique action on the jet and is a distinct and reproducible effect.

A series of sample photographs shows best the effect of changing the nozzle type and size. Figure 3 shows a Type A nozzle with orifice diameter of 0.040 in., and Figure 4 shows a Type A nozzle with an orifice 0.030 in. in diameter. The smooth water jet seems to explode suddenly and violently, and repeated photographs show that the location of the disintegration varies rapidly and randomly from 0.1 to 0.5 in. downstream from the orifice for the larger jet. The smaller jet disintegrates further downstream and in a manner which cuts the jet into distinct sections which disintegrate more slowly. The center of Figure 4 is about 1 in. from the nozzle.

Figure 5 shows a jet from a Type B nozzle 0.031 in. in diameter, and Fig-

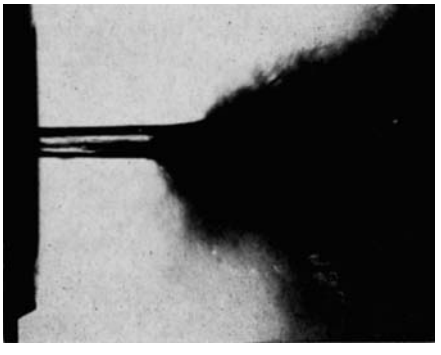

Fig. 3. Flashing jet 10X. Type A, D = 0.040 in., P = 120 lb./sq. in. T = 286°F.

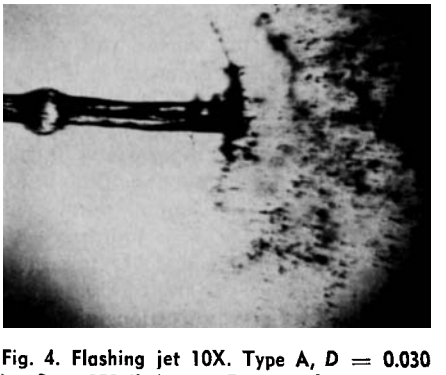

Fig. 4. Flashing jet 10X. Type A, D = 0.030 in., P = 131 lb./sq. in. T = 287°F. One inch from orifice.

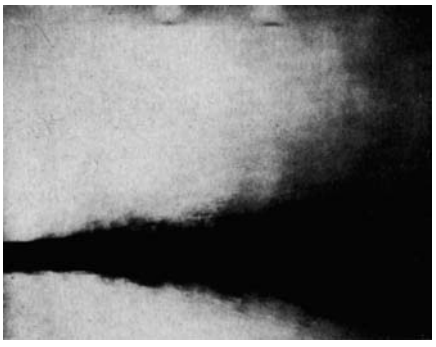

Fig. 5. Flashing jet 10X. Type B, $D = 0.031$ in., $P = 120$ lb./sq. in. $T = 295°F$.

ure 6 shows a jet from a Type B nozzle 0.020 in. in diameter. The larger jet of Figure 5 is typical of the shattering occurring in the jet from such a rough nozzle, and Figure 6 shows the effect of a temperature just below the shattering temperature.

The Type C nozzle is not shown because its extremely rough surface disintegrated even a cold jet, although irregularly, and the effect of flashing is not apparent in the photographs.

The rough nozzles show disintegration beginning at the nozzle discharge, and the sharp-edged orifices give a delayed action, with disintegration setting in several diameters downstream. This difference is explained on the basis of nucleation. As the hot water passes through the nozzle and the pressure decreases until enough driving force is established to form a bubble, the molecular arrangement in the liquid controls the nucleation of the bubble. The rough orifice has sufficient length to permit the surface irregularities to form low-pressure eddies. These eddies are shed regularly, move downstream as part of the jet, and serve as low-pressure stagnation spots which may well nucleate bubbles. The sharp-edged orifice offers no such opportunity, and the bubble formation is much like that of a bumping liquid in a boiling flask, with a sudden violent eruption of the bubbles.

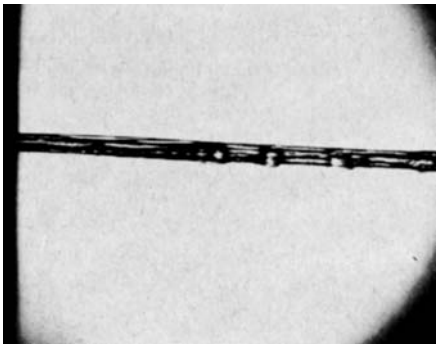

Fig. 6. Flashing jet 10X, Type B, $D = 0.020$ in., $P = 120$ lb./sq. in. $T = 284°F$.

A bubble is subject to three forces: the pressure on the liquid P_o, the vapor pressure in the bubble P_v, and the pressure exerted by the interfacial tension. The interfacial tension causes a pressure of $2\sigma/r$. For a bubble to grow in a superheated liquid the pressure acting outward must exceed those acting inward, or

$$P_v > P_o + \frac{2\sigma}{r}$$

The smallest bubble capable of growth is that one whose radius r_o just satisfies the equation

$$P_v = P_o + \frac{2\sigma}{r_o}$$

or

$$r_o = \frac{2\sigma}{P_v - P_o}$$

Since the vapor pressure is a function of the liquid temperature, then the minimum bubble radius can be calculated as a function of temperature and is shown in Table 2. Since the roughness in the Type B nozzles is of the order of 0.5 μ, then a temperature of about 270°F. would reduce the minimum radius to the order of the roughness in the orifice, and the eddies might be influential.

The bubble must continue to grow if it is to disrupt the jet, and the growth rate will determine the shattering effect it will have. Plesset and Zwick (6) and Forster and Zuber (7) have studied the growth rate and solved the mathematical system by different techniques to arrive at the same results. The bubble grows initially at a very rapid rate because of the rapid relaxation of the surface-tension pressure and the slow decrease in temperature of the liquid surrounding the bubble. In a few microseconds the bubble is about ten times its initial radius, the amount of liquid vaporized to fill the bubble cools the remaining liquid at the surface, and heat conduction becomes dominant. The radius then follows the relation

$$r = r_1 + C\,t^{1/2}$$

The bubble growth-rate constant was developed by Forster and Zuber to be

$$C = \left(\frac{C_p \Delta T}{L}\right)\left(\frac{\rho_2}{\rho_1}\right)(\pi D_{th})^{1/2}$$

The first grouping in the parentheses is the weight-fraction flashing at the saturation temperature and lower pressure, the second parenthesis encloses the specific-volume ratio of gas to liquid, and their product is then the volumetric increase upon flashing. The last term is a measure of the rate of heat conduction from the liquid to the vapor. Larger values of the growth-rate constant would indicate more rapid disintegration of the liquid mass.

Calculated values of the growth-rate constants are shown in Figure 7 for four different fluids. Water has a growth rate more than twice as large

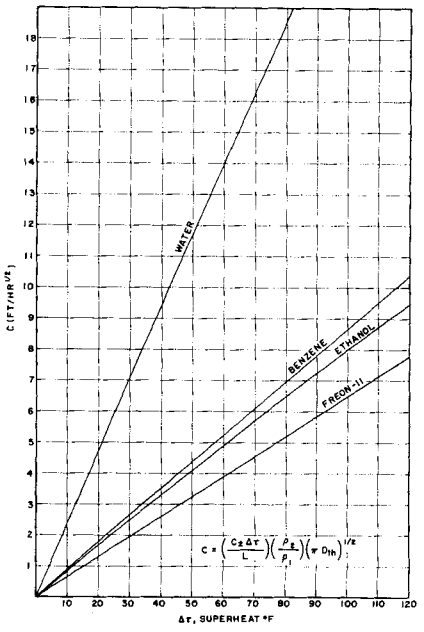

Fig. 7. Bubble growth-rate constants for superheated systems at 1 atm.

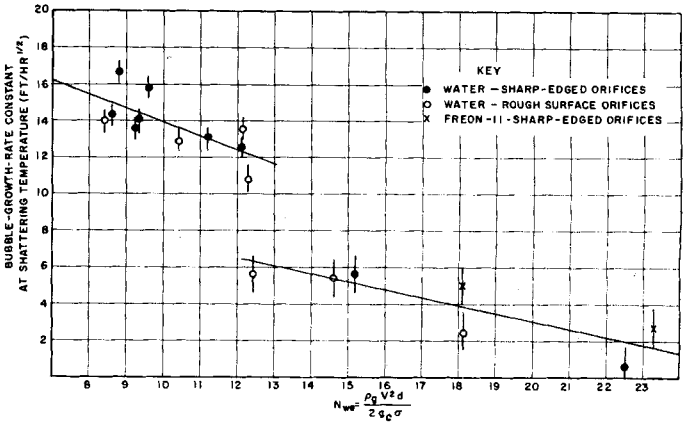

Fig. 8. Effect of Weber number on water and Freon-11 jet breakup.

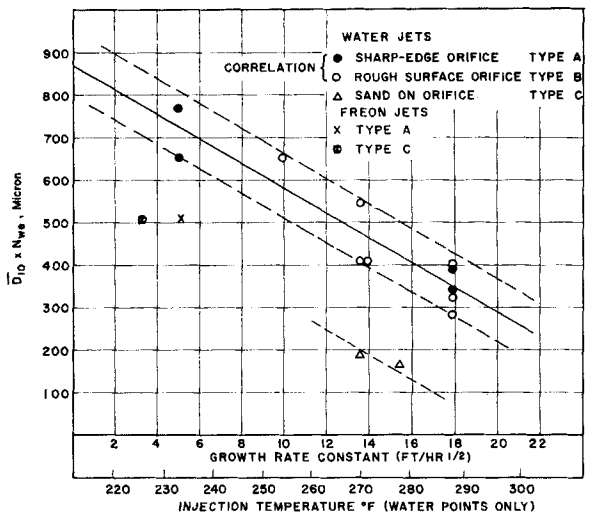

Fig. 9. Effect of bubble growth rate and Weber number on drop sizes.

as the organic compounds, when compared at the same superheat.

The analogy between thermal diffusivity and molecular diffusivity immediately brings forth the parallel concept of flashing from super-saturated liquids as well as super-heated liquids. The values of molecular diffusivity are an order of magnitude lower however, and the corresponding growth-rate constants are about one tenth as large as for superheated liquids. One experiment was attempted on cold water through which carbon dioxide was bubbled for 20 min. at 90 lb./sq. in. gauge. If saturation was attained, about 1% of the liquid volume would be flashed off. This system showed breakup almost identical with that of water containing no dissolved gas, which would be expected if the growth-rate constant was too low to influence breakup. Water at a superheat sufficient to cause flashing of 1% of the volume easily shattered a jet.

Observation and the data bring out the fact that a jet of large diameter may shatter at a superheat for which a smaller jet does not shatter. This brings in the possibility that jet stability may be an important factor; therefore the Weber number was determined for each system studied. The temperature at which each jet shattered permitted calculation of the Weber number and the growth-rate constant for each fluid system, with the result shown in Figure 8. Higher values of the Weber number permit shattering to occur with less superheat at the same flow velocity, giving smaller growth-rate constants. A Weber number of 12.5 is critical, with lower values of the Weber number requiring a significantly higher growth rate for shattering. This usually requires higher superheat.

The two straight lines representing the data best have the equations

$$C = 19.7 - 0.58\,N_{We} \text{ for } N_{We} < 12.5$$

$$C = 11.5 - 0.42\,N_{We} \text{ for } N_{We} > 12.5$$

An interesting aspect of Figure 8 is the lack of influence of roughness on the relationship, with close agreement for data for both kinds of orifice. This is in contrast to the marked difference in breakup seen in the photographs.

SPRAY CHARACTERISTICS

The drop sizes in the spray at a distance of 6 in. from the nozzle are given in Table 3. The four different mean drop sizes were computed from

$$\overline{D_{mn}} = \left[\frac{\Sigma\, D_i^{\,m}\,\Delta N_i}{\Sigma\, D_i^{\,n}\,\Delta N_i}\right]^{1/m-n}$$

Thus $\overline{D_{10}}$ is the linear mean diameter, $\overline{D_{20}}$ the surface mean diameter, $\overline{D_{30}}$ the volume mean diameter, and $\overline{D_{32}}$ the volume-surface mean diameter.

The corresponding dimensions of the orifice and the jet itself are given in Table 3, along with temperatures,

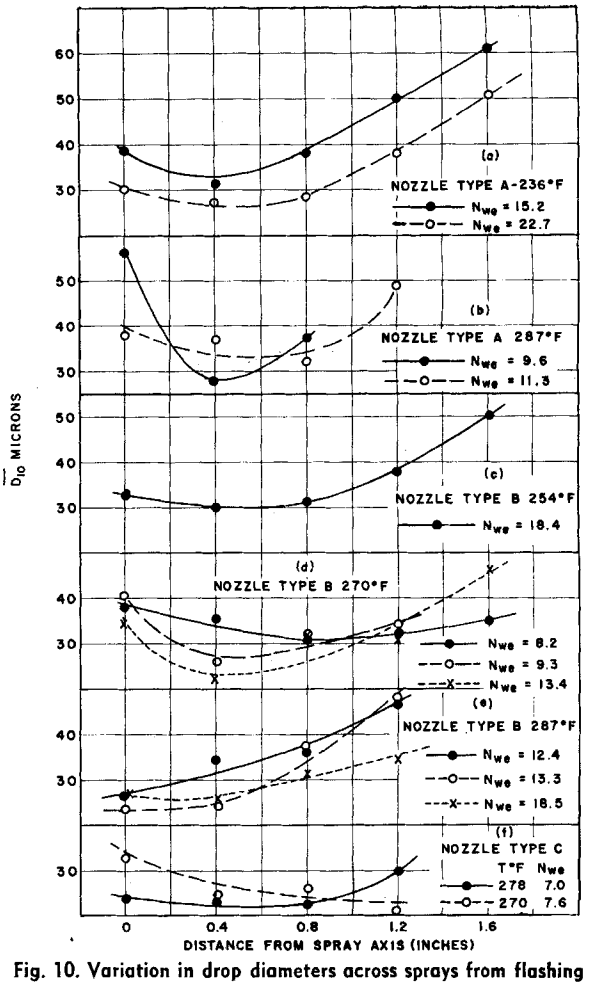

Fig. 10. Variation in drop diameters across sprays from flashing water jets.

TABLE 3. MEAN DROP SIZES

Run No.	Nozzles Type	D, in.	Jet D, in.	Jet Conditions T°F	ΔP	N_{We}	C, ft/hr$^{1/2}$	Liquid	Mean Drop-Sizes (microns) δ	$\overline{D}_{10}$	$\overline{D}_{20}$	$\overline{D}_{30}$	$\overline{D}_{32}$
1	A	0.040	0.032	287	120	11.3	17.9	H_2O	1.39	34.7	43.2	48.9	62.9
2	B*	0.031	0.031	287	120	11.0	17.9	"	1.39	54.5	59.8	64.3	74.5
3	A	0.080	0.066	204	80	14.9		"	0.88	142	186	227	336
4	A	0.080	0.066	236	80	15.2	5.0	"	1.22	43.0	50.9	59.6	82.2
5	A	0.080	0.066	236	120	22.7	5.0	"	1.43	33.9	39.4	44.9	58.3
6	A	0.030	0.025	287	130	9.57	17.9	"	1.49	35.7	45.6	62.6	85.1
7	B	0.031	0.031	287	90	8.21	17.9	"	1.71	34.3	40.0	48.7	71.9
8	B	0.040	0.035	270	130	13.3	13.6	"	1.77	30.7	34.9	39.4	50.0
9	B	0.040	0.035	287	90	9.27	17.9	"	1.62	35.0	38.4	41.9	49.6
10	B	0.040	0.035	287	130	13.4	17.9	"	1.69	29.8	33.9	35.7	39.4
11	B	0.060	0.053	254	120	18.4	9.9	"	1.21	35.6	42.9	52.0	76.3
12	B	0.060	0.053	270	80	12.4	13.6	"	1.67	32.7	37.4	44.1	61.2
13	B	0.060	0.053	270	120	18.5	13.6	"	1.53	29.6	33.6	38.0	48.5
14	C	0.020	0.020	80	94	5.14		"	0.73	82.3	118	197	280
15	C	0.020	0.020	270	130	7.56	13.6	"	1.95	25.1	27.4	30.4	38.9
16	C	0.020	0.020	278	120	7.03	15.4	"	1.60	24.2	27.1	30.0	36.6
17	A	0.030	0.025	152	94	18.1	5.0	F-11	1.66	28.5	32.4	36.0	44.4
18	C	0.020	0.020	125	95	14.1	3.2	F-11	1.16	36.1	43.4	55.0	84.5

bubble growth-rate constants, and Weber numbers.

The uniformity parameter, also shown in Table 3, is derived from a log-normal probability plot of the data for each analysis and is defined as

$$\delta = 0.394/\log_{10}(D_{90}/D_{50})$$

where D_{90} and D_{50} are the diameters read from the plot for cumulative percentages of 90 and 50, respectively. The size distribution fits the log-normal probability function as well as any other spray data.

The two lines in Table 3 for water below its boiling point show the poor breakup to be expected from such low-pressure orifice injection, even with the artificially roughened Type C nozzle, which tends to tear the stream into irregular masses because of its roughness alone.

Comparison of the mean drop sizes with those for other types of spray devices is only approximate, since injection conditions are quite significant for many devices. In general the flashing of water through these orifices produced a spray roughly similar to that from a swirl-chamber nozzle, somewhat larger in mean drop size than for gas atomized sprays, and somewhat smaller than the spray produced by most spinning-disk units. The mass fraction of the liquid flashed upon emerging from the nozzle can be computed from the first term of the bubble growth-rate constant and ranges up to a maximum of 7.8% (at 287°F.) for water. This compares favorably with the need for 0.5 to 1.0 lb. of air needed per pound of water in many gas-atomizing nozzles.

The uniformity parameters averaged 1.55 for a range of 1.21 to 1.95. This may be compared with typical values for other devices (8):

Gas atomizer:	$\delta = 0.93$
Spill-controlled swirl nozzle:	$\delta = 1.29$
Vaned-disk sprayer:	$\delta = 1.54$

Study of the data in Table 3 shows that the mean drop sizes decrease slightly with increasing Weber number at a given temperature and therefore at the same bubble growth-rate constant. A slight decrease is also indicated with increasing temperature and bubble growth-rate constant when the Weber number is approximately constant. These two trends suggested the best generalized correlation of drop sizes found, a plot of $(\overline{D_{10}} \cdot N_{We})$ vs. C, as shown in Figure 9. All water data for Type A and Type B nozzles fall in a reasonable band, but the Type C nozzle shows a smaller drop size and Freon-11 shows a smaller

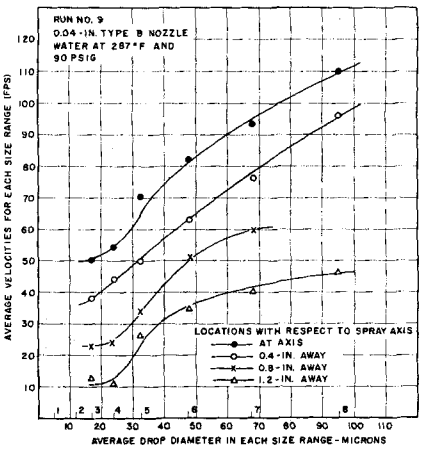

Fig. 11. Velocity of drops in a spray from flashing water jet 6 in. from the orifice.

value. The line through the band for water can be described by the equation

$$\overline{D_{10}}\,\mu = \frac{1{,}840 - 5.18\,T(°\text{F.})}{N_{We}}$$

The standard deviation is 6.1 %.

An attempt to correlate the uniformity parameter with the bubble growth-rate constant failed to show any significant relationship.

Drop-size analyses at different locations across the spray showed a trend of increasing drop size with distance from the spray axis. This is shown in Figure 10, in which the effect of Weber number is indicated for each nozzle type at various temperatures. The larger drops apparently migrate away from the center because of their inertia and the radial component added to the drops by the explosive flashing This effect is less evident when the Weber number is below the critical.

The velocities of the drops at the 6-in. distance are shown in Figure 11 for the different drop sizes at different locations across the spray. The smaller drops appear to have reached the multiphase flow velocity at that distance, and the decreasing velocities with increasing distance from the spray axis represents the velocity gradient to be expected in such a multiphase system.

The spray pattern was one of rapid expansion to a diameter of 3 to 4 in., with no significant expansion evident beyond the 6-in. distance chosen for our analytical point. Evaporation is rapid beyond the 6-in. distance however, with practically all of the drops disappearing within 4 to 5 ft. from the nozzle.

CONCLUSIONS

Flashing is an effective technique for producing sprays with a drop-size pattern similar to that produced by other devices. High pressures and high velocities are not necessary for the process, although superheating must be provided.

NOTATION

C	=	bubble growth-rate constant
C_p	=	heat capacity of liquid
D_i	=	average drop size in each size class in an analysis
$\overline{D_{mn}}$	=	mean drop size corresponding to chosen values of m and n
D_{th}	=	thermal diffusivity of liquid
d	=	diameter of liquid jet
g_c	=	conversion factor (poundals per pound force)
L	=	latent heat of vaporization
m, n	=	integer constants such that $m > n$
N_{We}	=	Weber number
P_o	=	pressure on system at free liquid surface
P_v	=	vapor pressure of liquid at its temperature T
r	=	radius of bubble at any time t
r_o	=	radius of smallest bubble capable of growth
r_1	=	radius of bubble when heat conduction begins to control ($r_1 \approx 10\,r_o$)
t	=	time from bubble radius r_1
V	=	velocity of jet relative to gas medium

Greek Letters

ΔN_i	=	number of drops in each size class in an analysis
ΔT	=	superheat
δ	=	uniformity parameter in drop size distribution
ϵ	=	height of roughness projection
ρ_g	=	density of gas phase surrounding jet
ρ_1	=	density of vapor
ρ_2	=	density of liquid
σ	=	surface tension

LITERATURE CITED

1. Brown, Ralph, Ph.D. thesis, Univ. Michigan, Ann Arbor, Michigan (1960).
2. Rayleigh, Lord, *Proc. London Math. Soc.*, **10**, 4 (1878).
3. Weber, C., *Zeit. fur Angew. Math.*, **11**, 106 (1931).
4. Hinze, J. O., *A.I.Ch.E. Journal*, **1**, 289 (1955).
5. York, J. L., and H. E. Stubbs, *Trans. Am. Soc. Mech. Engrs.*, **74**, 1157 (1952).
6. Plesset, M. S., and S. A. Zwick, *J. Appl. Phys.*, **25**, 492 (1954).
7. Forster, H. K., and N. Zuber, *ibid.*, p. 474.
8. Ranz, W. E., *Dept. Eng. Res., Bull No. 65*, The Pennsylvania State Univ., State College, Pennsylvania (1956).

Manuscript received December 29, 1960; revision received July 31, 1961; paper accepted August 14, 1961. Paper presented at A.I.Ch.E. New Orleans meeting.